

# Towards a Simplified Dynamic Model of the Actuation Capabilities of Legged Robots

Romeo Orsolino<sup>1</sup>, Michele Focchi<sup>1</sup>, Darwin G. Caldwell<sup>1</sup> and Claudio Semini<sup>1</sup>

## I. INTRODUCTION

Simplified dynamic models have found a wide diffusion in the research community of legged locomotion thanks to the good trade-off between descriptive accuracy and computational cost that they guarantee.

Among the most successful templates we can recall the Linear Inverted Pendulum (LIP) model and the Spring Loaded Inverted Pendulum (SLIP) model. Each of these templates, coupled with a suitable stability criterion such as the Zero Moment Point (ZMP) [1], the Capture Point (CP) or the limit cycle stability analysis, has represented a critical improvement towards the understanding of human locomotion and a step forward towards the realization of more and more natural gaits of legged robots.

The above mentioned templates focus on the balancing problem intended as a fight against gravity: the main goal is to accomplish the desired velocity, considering the unilateral nature of the contact forces.

## II. FEASIBILITY CONSTRAINTS

Such simplified models, however, ignore other physical phenomena that might hinder the motion execution such as the friction coefficients, the kinematic joint limits and the actuators limits. When one of these constraints is violated, indeed, the corresponding physical quantity is usually saturated to its maximum feasible value (maximum constant force in the case of the contact forces violation, maximum position in the case of the joint position limits or maximum torque in the case of the joint torque limits). If the feedback controller is not aware of such limits, this will result in an undesired feedforward control action (saturated constant input) and in a potential failure of the all motion plan.

These feasibility constraints have been considered at the control level in multiple manners, mainly resorting to the full kinematics of the system [2]. However, we still miss the ability to devise *online* motion plans that can verify these constraints over longer horizons and possibly adapt the plans according to these requirement with large notice, hence the need of resorting to *offline* machine learning [3]. With the increasing complexity of the motions that our robot are expected to perform, taking these restrictions into account sufficiently in advance becomes of even greater importance.

This work was supported by Istituto Italiano di Tecnologia.

<sup>1</sup>Department of Advanced Robotics, Istituto Italiano di Tecnologia, Genova, Italy. email: {romeo.orsolino, michele.focchi, darwin.caldwell, claudio.semini}@iit.it

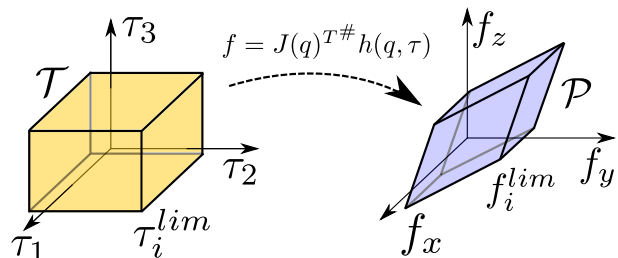


Fig. 1. The mapping between joint torques and end effector forces. In this example the dimension of the torques space  $\dim(\mathcal{T}) = n = 3$  is equal to the dimension of the manifold of the contact forces  $\dim(\mathcal{P}) = m = 3$ .

In the following section of this manuscript we focus on the problem of joint actuation limits and we describe the properties of the *actuation polygons*, or *force polygons*, and how they can be obtained.

## III. ACTUATION POLYGONS

The dynamic equation of motion can be expressed in the following generalized form:

$$\mathbf{M}(\mathbf{q})\ddot{\mathbf{q}} + \mathbf{c}(\mathbf{q}, \dot{\mathbf{q}}) + \mathbf{g}(\mathbf{q}) = \boldsymbol{\tau} + \mathbf{J}_s^T(\mathbf{q})\mathbf{f} \quad (1)$$

which includes both the Degrees of Freedom of the unactuated floating base and the actuated joints. The same relation can be expanded in two lines in order to explicitly highlight these two terms:

$$\begin{bmatrix} \mathbf{M}_b & \mathbf{M}_{bj} \\ \mathbf{M}_{bj}^T & \mathbf{M}_j \end{bmatrix} \begin{bmatrix} \dot{\mathbf{v}} \\ \ddot{\mathbf{q}}_j \end{bmatrix} + \begin{bmatrix} \mathbf{c}_b \\ \mathbf{c}_j \end{bmatrix} + \begin{bmatrix} \mathbf{g}_b \\ \mathbf{g}_j \end{bmatrix} = \begin{bmatrix} \mathbf{0}_{6 \times n} \\ \mathbf{I}_{n \times n} \end{bmatrix} \boldsymbol{\tau} + \begin{bmatrix} \mathbf{J}_{sb}^T \\ \mathbf{J}_j^T \end{bmatrix} \mathbf{f} \quad (2)$$

We now deliberately neglect the first line (related to the floating base) and thus discard the coupling term  $\mathbf{J}_{sb}^T$  that describes the interaction among the legs.

In this way we can then rearrange Eq. 2 above to explicitly express the contact forces  $\mathbf{f}$ :

$$\mathbf{f} = \mathbf{J}_j^{T\#} \underbrace{(\mathbf{M}(\mathbf{q})\ddot{\mathbf{q}} + \mathbf{c}(\mathbf{q}, \dot{\mathbf{q}}) + \mathbf{g}(\mathbf{q}) - \boldsymbol{\tau})}_{\mathbf{h}(\mathbf{q}, \boldsymbol{\tau})} \quad (3)$$

The definition of the function  $\mathbf{h}(\mathbf{q}, \boldsymbol{\tau})$  may vary depending on the assumptions we take about the motion. For example we may assume a quasi-static motion ( $\mathbf{q} = \dot{\mathbf{q}} = 0$ ) and we would then get in this way:  $\mathbf{h}(\mathbf{q}, \boldsymbol{\tau}) = \mathbf{g}(\mathbf{q}) - \boldsymbol{\tau}$ .

In the next paragraph we will deal with the problem of the inversion of the transposed leg Jacobian  $\mathbf{J}_j^T$  term and treat it into two different ways depending on the legs redundancy.

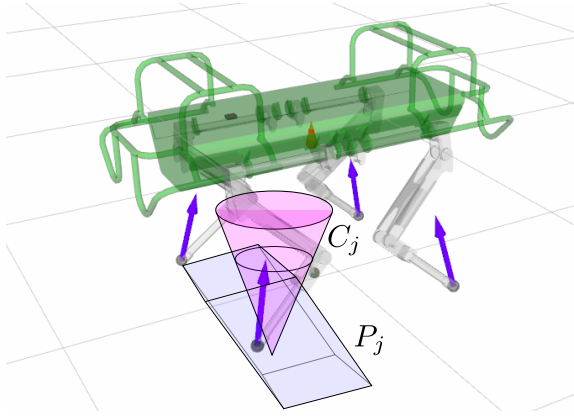


Fig. 2. Representation of the friction cone  $C_j$  and actuation polygon  $P_j$  on one foot of the HyQ robot ( $j$  is the leg index). The purple arrows represent the contact forces.

### A. Inversion of the Transposed Jacobian term

For each branch  $j$  of the floating base system we have a limb Jacobian matrix  $\mathbf{J}_j^T \in \mathbb{R}^{n \times m}$  where  $n$  is the number of actuated joints of limb and  $m$  is the dimension of the contact wrench at the end effector.

For non redundant limbs ( $n = m$ ) the matrix  $\mathbf{J}_j^T$  is invertible and thus  $\mathbf{J}_j^{T\#}$  corresponds to the inverse of  $\mathbf{J}_j^T$ . Eq. (3) can be written in this case as:  $\mathbf{f} = \mathbf{J}_j^{-T} \mathbf{h}(\mathbf{q}, \boldsymbol{\tau})$ .

In the generic case of redundant limbs, however, we have that  $n > m$  and  $\mathbf{J}_j^T$  is not invertible. One first option in this case consists in using the Moore-Penrose pseudo-inverse:

$$\mathbf{J}_j^{T\#} = ((\mathbf{J}_j^T \mathbf{J}_j)^{-1} \mathbf{J}_j^T)^T = \mathbf{J}_j (\mathbf{J}_j^T \mathbf{J}_j)^{-T} \quad (4)$$

This choice corresponds to minimizing  $\|\mathbf{J}_j^T \mathbf{f} - \boldsymbol{\tau}\|_2^2$ . This quantity will be zero, and thus the inversion given by Eq. (4) will be accurate, only if the joint torque/force  $\boldsymbol{\tau}$  belongs to the pre-image of  $\mathbf{J}_j^T$ , i. e.  $\boldsymbol{\tau} \in \text{Im}(\mathbf{J}_j^T)$ .

As an alternative, the method proposed in [4], for the case of redundant manipulators, consists in solving, at most,  $\frac{2n!}{(2n-m)!m!}$  systems of linear equations in order to find the set of force polytope vertices that make sure the joint torques respect this condition.

### B. Actuation polygons computation

So far we have explained how a set of joint torques can be mapped into an equivalent contact force at the end-effector. We can now use Eq. (3) to compute the maximum and minimum contact forces that the  $i$ -th limb can exert on the environment, considering its own actuation limits:

$$\mathbf{f}_i^{lim} = \mathbf{J}_j^{T\#} \cdot \mathbf{h}(\mathbf{q}, \boldsymbol{\tau}_i^{lim}), \quad i = 1, \dots, 2^n \quad (5)$$

$\boldsymbol{\tau}_i^{lim} \in \mathbb{R}^n$  is a vector containing a combination of upper and lower bounds of the joint torques (see Fig. 1). The resulting  $2^n$  values of  $\mathbf{f}_i^{lim}$  represent the vertices of the force/actuation polygon  $\mathcal{P}_i$  of the considered limb:

$$\mathcal{P}_j = \left\{ \mathbf{f} \in \mathbb{R}^m \mid \mathbf{f} = \mathbf{J}_j^{T\#} \cdot \mathbf{h}(\mathbf{q}, \boldsymbol{\tau}), \quad \boldsymbol{\tau} \in \mathcal{T} \right\} \quad (6)$$

The actuation polygon  $\mathcal{P}_j$  can then be intersected with the friction cone  $C_j$  to obtain the set of all the contact forces that

simultaneously respect both the friction cone constraints and the joint actuation limits of the  $j$ -th limb (see Fig. 2).

Examples of how such quantities can be exploited in the field of Model Predictive Control and motion planning can be found in [5] and [6].

## IV. SIMPLIFIED DYNAMIC MODELS

The actuation polygons can be used to capture phenomena which cannot otherwise be observed by the friction cones alone. These phenomena include the relation between foot placement and the maximal contact force that the robot can exert on the ground and how the configuration affects this.

In [6] we have shown that the actuation polygons can be used to map the joint force/torque limits into *Actuation Wrench Polytope* (AWP) constraints to restrict the overall wrench acting on Center of Mass (CoM) of the robot. The used method is comparable to the way friction cones can be mapped into *Contact Wrench Cone* (CWC) constraints to limit the overall wrench allowed to act on the robot [7].

Combined, for example, with the use of *centroidal dynamics* [8], CWC and AWP constraints represent a solid example of how actuation polygons can be employed for the definition of new control and motion planning policies for legged robots.

## V. CONCLUSION

In this manuscript we have described the required steps for the computation of the actuation polygons and the strong analogies with the well known friction cones.

We believe that the force polygons represent an important tool that we may exploit in the future for the definition of new simplified dynamic models and for the generation of more physically feasible motion plans for legged robots.

## REFERENCES

- [1] S. Kajita, F. Kanehiro, K. Kaneko, K. Fujiwara, K. Harada, K. Yokoi, and H. Hirukawa, "Biped walking pattern generation by using preview control of zero-moment point," *IEEE International Conference on Robotics and Automation (ICRA)*, pp. 1620–1626, 2003.
- [2] H. Dai, A. Valenzuela, and R. Tedrake, "Whole-body Motion Planning with Simple Dynamics and Full Kinematics," *International Conference on Humanoid Robots*, no. JANUARY 2014, pp. 295–302, 2014.
- [3] J. Carpentier, N. Mansard, J. Carpentier, N. Mansard, M.-c. Locomotion, L. Robots, R. Laas, J. Carpentier, S. Member, and N. Mansard, "Multi-contact Locomotion of Legged Robots To cite this version : Multi-contact Locomotion of Legged Robots," *IEEE Transactions on Robotics*, no. August, pp. 0–21, 2018.
- [4] P. Chiacchio, Y. Bouffard-Vercelli, and F. Pierrot, "Force Polytope and Force Ellipsoid for Redundant Manipulators," *Journal of Robotic Systems*, vol. 14, no. 8, pp. 613–620, 1997.
- [5] V. Samy, K. Bouyarmane, and A. Kheddar, "Adaptive Compliance in Post-Impact Humanoid Falls Using Preview Control of a Reduce Model," *IEEE-RAS International Conference on Humanoid Robots*, 2017.
- [6] R. Orsolino, M. Focchi, C. Mastalli, H. Dai, D. G. Caldwell, and C. Semini, "Application of Wrench based Feasibility Analysis to the Online Trajectory Optimization of Legged Robots," *IEEE Robotics and Automation Letters (RA-L)*, vol. 3, no. 4, pp. 3363–3370, 2017.
- [7] H. Dai and R. Tedrake, "Planning robust walking motion on uneven terrain via convex optimization," *2016 IEEE-RAS International Conference on Humanoid Robots (Humanoids 2016)*, 2016.
- [8] D. E. Orin, A. Goswami, and S. H. Lee, "Centroidal Dynamics of a Humanoid Robot," *Autonomous Robots (AURO)*, vol. 35, pp. 161–176, 2013.